Self-diffusion coefficients and shear viscosity of model nanocolloidal dispersions by molecular dynamics simulation

María J. Nuevo and Juan J. Morales*
Departamento de Física, Facultad de Ciencias, Universidad de Extremadura, 06071 Badajoz, Spain

David M. Heyes
Department of Chemistry, University of Surrey, Guildford GU2 5XH, United Kingdom
(Received 15 May 1998)

The self-diffusion coefficients D of both species in model nanocolloidal dispersions have been computed using molecular dynamics (MD) simulation, in which three-dimensional model spherical colloidal particles were in a molecularly discrete solvent. The effects of the relative density, size, and concentration of the two species were explored. Simulations were carried out at infinite dilution (a single colloidal particle) and at finite packing fractions (many colloidal particles) in the simulation cell using single interaction centers between the model colloidal particles and solvent molecules. The calculations used the Weeks-Chandler-Andersen (WCA) or Lennard-Jones (LJ), interaction potentials between all species. Nanocolloid particles with diameters up to ~6 times the solvent molecule were modeled. At liquidlike densities the self-diffusion coefficients of the colloidal particles, D_c, for all sizes and packing fractions, statistically exhibited no mass dependence but a significant colloid particle size dependence. This can be interpreted in a systematic manner using a Mori series expansion. The first Mori coefficient (which is inversely proportional to particle mass) dominates the value of the self-diffusion coefficient for both species, and which also leads to a formal cancellation of the mass dependence at the order of the first Mori coefficient K_{B1} (the self-diffusion coefficient is therefore determined by a ''static'' property to this order). The values of D_c at each packing fraction are found to be approximately inversely proportional to the colloidal particle diameter, quantitatively following the same trend as the Stokes-Einstein equation, even for the small colloidal particle sizes and finite colloidal particle concentrations studied here. Another consequence of the dominance of the first Mori coefficient is that the normalized velocity autocorrelation function of the colloidal particle at a short time can be represented well at all state points and packing fractions by the analytic form $\simeq\cos(\Omega_0 t)$, where $\Omega_0=\sqrt{K_{B1}}$, which is the so-called Einstein frequency. LJ and WCA systems with otherwise the same system parameters manifest the same oscillation frequency, but the LJ oscillation amplitudes are larger and the values of D_c are smaller. The self-diffusion coefficients and shear viscosities obey a volume fraction dependence similar to that found for much larger colloidal particles. [S1063-651X(98)15211-X]

PACS number(s): 66.10.−x, 82.20.Tr, 82.20.Wt

I. INTRODUCTION

Colloidal liquids consist of solid particles typically 0.1–1.0 μm in diameter, suspended in a ''host'' liquid [1]. The ratio of the mass of the colloidal particle, m_c, and solvent molecule, m_s, is for all practical purposes in the $m_c/m_s\to\infty$ limit for colloidal particles in this range. The size ratio of the two species rather than the mass ratio is the important parameter determining the dynamical behavior of importance to transport coefficients, as inertial effects are not significant for the low Reynolds number flows typically found in many colloidal liquid flow situations. The complexity of these systems prohibits exact analytic treatments of their dynamical properties in all but the most idealized of cases (e.g., infinitely dilute systems), and alternative analytical treatments or numerical simulation techniques which treat the faster degrees of freedom in an approximate way are required at finite concentration. There are now a number of ''mesoscale'' discrete particle simulation techniques that have been developed with varying degrees of rigor, such as Brownian dynamics [2,3], which is the most simple model in having no many-body hydrodynamics, i.e., correlated colloid particle trajectories caused by the flow field they establish in the intervening solvent. Stokesian dynamics, which incorporates partially the many-body hydrodynamics, can be cast (mainly) in the diffusion tensor [4–6] or resistance tensor formulations [7]. These techniques are inadequate in dealing with the dynamical behavior of *nanocolloidal* particles, where the inertia of both colloid and solvent molecules are important, and where both species relax over similar time scales. The nanocolloids provide interesting transitional states between simple molecular liquids and the more usual *macrocolloids* in which the colloid particle diameters are typically in excess of ~0.1 μm. Previously, molecular dynamics (MD) simulations of single so-called Brownian particles (which are nanocolloids at infinite dilution) were carried out to investigate the mass and size dependence of the self-diffusion coefficient. These data have been interpreted within the framework of the Mori series expansion, e.g., Refs. [8–12]. One of the important conclusions from these studies is the relative insensitivity of the self-diffusion coefficient of the colloidal particle to its mass, but the extreme sensitivity to its size. In this study, we continue to explore the consequences of this, in particular for the analytic form

*Deceased.

of the velocity autocorrelation function. The effects of finite colloid particle concentrations on the behavior of the self-diffusion coefficient are also considered here.

II. THEORETICAL BACKGROUND

Transport coefficients calculated using the Green-Kubo (GK) integral formulas require appropriate correlation functions which can be calculated by a MD computer simulation [13]. The self-diffusion coefficient D_i for particle i can be obtained using the velocity autocorrelation function $C_{Vi}(t)$ in the GK integrand,

$$C_{Vi}(t)=\langle \mathbf{v}_i(t)\cdot\mathbf{v}_i(0)\rangle, \tag{1}$$

where $\mathbf{v}_i$ is the velocity of particle i and $\langle\cdots\rangle$ denotes an average over time origins. The time-dependent self-diffusion coefficient of particle i is given by

$$D_i(t)=(1/3)\int_0^t\left(1-\frac{x}{t}\right)C_{Vi}(x)dx, \tag{2}$$

and the transport coefficient is $D_i=\lim_{t\to\infty}D_i(t)$. The self-diffusion coefficient of particle i can also be obtained directly by MD from the linear region of the mean-square displacement as [13–16]

$$D_i=\lim_{t\to\infty}\frac{\langle|\mathbf{r}_i(t)-\mathbf{r}_i(0)|^2\rangle}{6t}, \tag{3}$$

where $\mathbf{r}_i(t)$ is the absolute position of particle i at a time t after an arbitrarily defined time origin, and $\langle\cdots\rangle$ again denotes an average over time origins. Approximate expressions for the transport coefficients can be written using the generalized Langevin equation, (GLE) formulation for the time correlation function in terms of a hierarchy of memory functions. According to the GLE formalism, the diffusion coefficient for an arbitrary species in the system can be obtained from the corresponding velocity autocorrelation function [17,18]

$$D=\frac{kT}{m}\int_0^\infty\frac{\langle\mathbf{v}(t)\cdot\mathbf{v}(0)\rangle}{\langle\mathbf{v}^2\rangle}dt=\frac{kT}{m\tilde{M}(0)}, \tag{4}$$

where m is the mass of the particle of interest, k is Boltzmann's constant, and $\tilde{M}(0)$ is the Laplace transform of the memory function at zero frequency, values of which can be expressed in terms of the Mori expansion and so-called Mori coefficients

$$\tilde{M}(s)=\frac{K_1}{s+K_2}\frac{s+K_3}{s+\cdots}, \tag{5}$$

where the memory kernels $K_n=M_n(0)$ are the Mori coefficients. For example, up to the fourth frequency moment or the second Mori coefficient, $K_{i=2}$, we have the generic form

$$\tilde{M}(0)=\int_0^\infty M(t)dt=\int_0^\infty K_1 f(K_2,t)dt. \tag{6}$$

where $f(K_2,t)$ is a function of K_2 and higher order Mori coefficients. The first, and to a lesser extent the second, Mori coefficient can be computed accurately using MD simulation. If there are $N_{\rm sp}$ molecules of a particular species in the simulation cell, the Mori coefficients can be obtained from the time average of the nth time derivative of the normalized velocity $\mathbf{v}_i$ as [19]

$$U_n=\frac{m}{N_{\rm sp}kT}\left\langle\sum_{i=1}^{N_{\rm sp}}\mathbf{v}_i^n\cdot\mathbf{v}_i^n\right\rangle. \tag{7}$$

For example the first two Mori coefficients are given by

$$K_1=U_1=\frac{1}{3N_{\rm sp}kTm}\left\langle\sum_{i=1}^{N_{\rm sp}}\mathbf{F}_i^2\right\rangle, \tag{8}$$

where $\mathbf{F}_i$ is the force on particle i, and

$$K_2=\frac{U_2}{K_1}-K_1. \tag{9}$$

In practice, the statistical uncertainty in K_i deteriorates rapidly with increasing i, and only K_1, and to a somewhat lesser extent K_2, can be computed with acceptable statistics when $N_{\rm sp}\sim 1$, as is the case for one of the species here. As an exact expression for the memory function is not known for simulation liquids, an assumption is often made about its analytic form. For example, according to Toxvaerd [20,21], as the isotope mass is increased, a Gaussian term in the memory function becomes the main contribution. The expression for the memory function in this approximation is

$$M(t)=K_1e^{-K_2t^2/2}, \tag{10}$$

which is therefore uniquely defined in terms of the first two Mori coefficients. Then,

$$\tilde{M}(0)=\int_0^\infty M(t)dt=\frac{K_1}{2}\sqrt{\frac{\pi}{K_2}}, \tag{11}$$

which takes the form of K_1 times a relaxation time, τ, composed of $\sim(K_2)^{-1/2}$ times a numerical constant $O(1)$. Therefore in the Gaussian memory function approximation to second order in the Mori coefficients the diffusion coefficient is using Eq. (11) substituted in Eq. (4):

$$D_G=\frac{\mathbf{k}T}{mK_1}\sqrt{\frac{2K_2}{\pi}}. \tag{12}$$

In the absence of an exact solution for the memory function in Eq. (4), many approximate closures of this continued fraction have been proposed and evaluated by comparing with molecular dynamics ''exact'' self-diffusion coefficients

(e.g., Refs. [12,14,15]). The important conclusion in the present context is that a truncation at the first Mori coefficient typically gives a reasonably good value for the self-diffusion coefficient, which is often not improved by going to higher Mori coefficients. As we will discuss, in practice, it is found that the relaxation time τ is only weakly dependent on mass.

As may be seen from Eq. (8), K_1 is the ratio of a configurational i.e., mass independent) or ''static'' average and the mass of the particle of interest, so that for solvent and colloid we expect

$$m_c K_{c1} f = m_s K_{s1}, \tag{13}$$

where m_c and m_s are the masses of the colloidal and solvent particles, respectively. K_{c1} and K_{s1} are the corresponding first Mori coefficients. f is unity when the solvent and colloid particle are the same size i.e., $\sigma_c = \sigma_s$. It was shown in a previous simulation study that f is reasonably well approximated by a simple function of σ_c/σ_s in two and three dimensions, which reflects the increased number of neighbors and resulting greater value for K_1 for the larger solute particles [9]. Let D_c and D_s be the self-diffusion coefficients of the colloidal particle and the solvent particle, respectively. The insensitivity of D_c to the mass of the colloidal particle is a direct consequence of the dominance of the first Mori coefficient

$$\begin{aligned} D_c &= (kT/m_c)/\tilde{M}(0) \approx (kT/m_c)/(\tau K_{c1}) \\ &= kT/\tau g(\sigma_c, \sigma_s, \rho_c, \rho_s), \end{aligned} \tag{14}$$

where ρ_c and ρ_s are the number densities of colloid and solvent particles, respectively, and g is a static average. The relaxation time τ is largely mass independent. The mass dependence comes in at the level of K_2. Tankeshwar showed that this puts an approximate bound of $1 < D_c(m_s)/D_c(m_c) < \sqrt{2}$ at infinite dilution in the colloidal particle for all state points [14], which is in accord with our previous simulation results on single colloidal particle systems [11].

The first Mori coefficient is also equal to the square of the so-called Einstein frequency, Ω_0, which is the frequency at which any molecule would vibrate if it were undergoing small oscillations in the average potential well produced by its surrounding molecules [16]. The short-time expansion of $C_V(t)$ for colloid or solvent particle is, in terms of Ω_0,

$$C_V(t) = \frac{kT}{m}\left(1 - \Omega_0^2 \frac{t^2}{2!} + \cdots\right). \tag{15}$$

Here we consider the dependence of the self-diffusion coefficients and shear viscosity on the mass, size, and concentration of the model nanocolloidal particles. The time dependence of the velocity autocorrelation function on mass and size of the colloidal particle is also considered.

III. COMPUTATIONAL DETAILS

The MD computer simulations had one or more colloidal particles in a cubic simulation box. The basic interaction law between all the particles was the purely repulsive Weeks-Chandler-Andersen (WCA), potential [22], which is a potential formed out of the repulsive part of the Lennard-Jones (LJ) potential shifted upwards by the minimum energy ϵ, and truncated at the potential minimum $r_m = 2^{1/6}\sigma$, where σ is the diameter of the particle. One of the advantages of the WCA potential is that it is short ranged and therefore the solvent can be computed relatively efficiently. The potential between colloid and solvent particle was modified to reflect the volume of the colloid particle [8],

$$u(r) = \begin{cases} 4\epsilon\left[\left(\dfrac{\sigma_s}{r-\alpha}\right)^{12} - \left(\dfrac{\sigma_s}{r-\alpha}\right)^{6}\right] + \epsilon & \text{for } r \leqslant r_m \\ 0 & \text{for } r > r_m. \end{cases} \tag{16}$$

This model for the colloid has been used by us before in previous publications (e.g., Ref. [11]). The advantage of this analytic form is that it shifts the potential out a further α in distance while retaining the same curvature as between two solvent molecules (i.e., when $\alpha = 0$) which minimizes any numerical algorithmic errors in updating the particle positions. The cutoff separation r_m for this potential is $r_m = \alpha + 2^{1/6}\sigma_s$. Colloid-colloid interactions were chosen to be the same as those between colloid and solvent molecules.

An alternative procedure would be to assign a diameter to the colloidal particle, σ_c, and to use the potential

$$u(r) = \begin{cases} 4\epsilon\left[\left(\dfrac{\sigma_{\rm cs}}{r}\right)^{12} - \left(\dfrac{\sigma_{\rm cs}}{r}\right)^{6}\right] + \epsilon & \text{for } r \leqslant r_m \\ 0 & \text{for } r > r_m, \end{cases} \tag{17}$$

and a typical combining rule for the diameters of the two species, such as $\sigma_{\rm cs} = (\sigma_c + \sigma_s)/2$ and $r_m = 2^{1/6}\sigma_{\rm cs}$. However, this would make the solvent-colloid interaction much steeper than between the solvent molecules for a colloidal particle diameter larger than that of the solvent molecule, which is unrealistic as any colloidal particle consists of atoms similar to those of the solvent in its periphery. Nevertheless, a comparison between these two potential forms allows us to relate α to an equivalent core diameter for the colloidal particle. That is, $\sigma_{\rm cs} \approx \sigma_s + \alpha$, which gives $\sigma_c \approx \sigma_s + 2\alpha$. Therefore the ratio of the volume of the colloidal particle relative to that of the solvent is approximately $[(\sigma_s + 2\alpha)/\sigma_s]^3$. Calculations were also performed with the same model but using the full Lennard-Jones model potential truncated at the appropriate value of 2.5σ for solvent-solvent, colloid-colloid, and colloid-solvent particles.

The Verlet algorithm was used [23], with the system kept at approximately constant temperature using velocity rescaling [24] or Nosé-Hoover [25–27] thermostats. The simulations were carried out at solvent reduced densities $\rho_s = N\sigma_s^3/V$ in the range 0.7–0.9 and at a reduced temperature

TABLE I. Details of the simulations containing one colloidal particle in the simulation cell i.e., in near infinite dilution limit or $\phi \to 0$. The simulations were carried out for $N_c = 1$ and $N_s = N - N_c$ solvent molecules using the WCA potential for all interactions. Key: α is the colloid size potential parameter from Eq. (16), m_c/m_s is the ratio of the mass of a colloid particle divided by that of a solvent molecule, D_c is the diffusion coefficient of the colloid particle, D_s is the diffusion coefficient of the solvent particle, η is the shear viscosity from the Green-Kubo formula taking all interactions into account [16], Ω_{c0} is the Einstein frequency of the colloidal particle from the first Mori coefficient for the colloid from Eq. (8), and Ω_{s0} is the Einstein frequency of the solvent from the first Mori coefficient for the solvent from Eq. (8). The cycle times are $\tau_{cs} = 2\pi/\Omega_{s0}$ and $\tau_{cc} = 2\pi/\Omega_{c0}$. The units are those of the solvent molecule: σ_c, ϵ, and m_s. In all simulations the solvent density was $\rho_s = 0.7$ and $kT/\epsilon = 1.0$. Typical statistical uncertainties in the colloid self-diffusion coefficients are ± 5 and $\pm 2\%$ for the solvent molecules.

ρ_s	N	m_c/m_s	α	Ω_{c0}	Ω_{s0}	τ_{cc}	τ_{cs}	D_c	D_s	η
0.7	1000	3.375	0.5	13.1	14.4	0.480	0.436	0.0517	0.127	0.848
0.7	1000	1.000	0.5	24.0	14.4	0.262	0.436	0.0612	0.128	0.810
0.7	2916	1.000	0.5	25.5	14.4	0.246	0.438	0.064	0.125	-
0.7	1000	0.296	0.5	44.2	14.4	0.142	0.436	0.0559	0.127	0.843
0.7	8000	1.000	1.0	33.7	14.4	0.187	0.438	0.0362	0.134	0.843
0.7	8000	0.296	1.0	62.0	14.4	0.101	0.438	0.0389	0.130	0.838
0.7	8000	1.000	1.5	43.7	14.4	0.144	0.437	0.0260	0.132	0.839
0.7	8000	1.000	2.0	53.4	14.5	0.118	0.435	0.0217	0.123	0.849
0.7	8000	1.000	2.5	64.1	14.5	0.098	0.432	0.0176	0.124	0.858
0.9	8000	1.000	0.5	34.2	20.0	0.184	0.315	0.0189	0.0474	3.07
0.9	8000	1.000	1.0	49.0	20.0	0.128	0.314	0.0108	0.0473	3.01
0.9	8000	1.000	1.5	63.8	20.1	0.098	0.313	0.0077	0.0471	3.05
0.9	8000	3.375	2.0	43.0	20.2	0.146	0.311	0.0061	0.0450	3.18
0.9	8000	0.296	2.5	107.1	20.4	0.059	0.309	0.0041	0.0434	3.31
0.9	8000	1.000	2.5	95.0	20.4	0.066	0.309	0.0045	0.0437	3.27
0.9	8000	3.375	2.5	51.7	20.4	0.122	0.309	0.0041	0.0436	3.19

of $kT/\epsilon = 1.0$. The time step was $h = 0.005\sigma_s(m_s/\epsilon)^{1/2}$, and the simulations extended typically for $\simeq 10^6$ time steps.

Simulations were carried out at infinite dilution (i.e., with a single colloidal particle in the simulation cell) and at finite packing fractions, ϕ (i.e., with many colloidal particles in the simulation cell), to investigate the effects of colloidal particle concentration on the diffusion coefficient, i.e., $D(\phi, \sigma_c)$ for a colloid packing fraction ϕ and colloidal particle size σ_c. We have $N = N_c + N_s$, where N, N_c, and N_s are the total number of particles, the number of colloidal, and the number of solvent particles, respectively. We chose systems up to $N = 10\,976$ to investigate the system size dependence of the self-diffusion coefficient of both species.

The establishment of a system at a given volume fraction is not trivial when $\sigma_s/\sigma_c \sim 1$ because of uncertain excluded volume effects between colloid and particle. The packing fraction of the model colloidal particles was defined to be

$$\phi = \frac{N_c}{V}\frac{\pi}{6}(\sigma_c + \sigma_s)^3, \tag{18}$$

with $(\sigma_c + \sigma_s)$ assumed to be the *effective* diameter of the colloidal particle, and V the total volume of the system. The number of solvent molecules was determined by ''filling'' the (assumed) usable space between the colloidal particles with N_s solvent molecules,

$$N_s = \rho_s V_s = \rho_s(V - V_c) = \rho_s V(1 - \phi), \tag{19}$$

where V_s is the volume available to the solvent. Equation (19) is only exact in the $\phi \to 0$ limit here, as σ_s and σ_c are the same order of magnitude, and therefore we are assuming that there are no overlapping regions of solvent exclusion around the colloidal particles. If we let $\sigma_s = 1$ then Eqs. (18) and (19) can be written in terms of α as

$$\phi = \frac{\rho_s N_c \pi (2+\alpha)^3}{6N_s + \rho_s N_c \pi (2+\alpha)^3} \tag{20}$$

and

$$N_s = \rho_s \frac{N_c \pi}{6\phi}(2+\alpha)^3(1-\phi) \tag{21}$$

to specify ϕ and α values and obtain the total size of the system to be simulated with the number of solvent molecules for a given number of colloidal particles being given by Eq. (21).

IV. RESULTS AND DISCUSSION

Several volume fraction values and colloidal diameter particle values were used in the simulations. Table I gives the data for WCA simulations carried out with a single col-

TABLE II. Details of the simulations carried out at finite colloid concentration with a finite colloid packing fraction, ϕ, using the WCA potential form for all pair interactions. Key: α is the colloid size potential parameter from Eq. (16), N_c is the number of colloidal particles, N_s is the number of solvent molecules computed from Eq. (19), K_{c1} is the first Mori coefficient of the colloidal particle from Eq. (8), K_{c2} is the second Mori coefficient of the colloidal particle from Eq. (9), and S is the cubic box side-length. Other parameters are as for Table I. The units are those of the solvent: σ_s, ϵ, and m_s. The asterisk indicates that an ambiguous limiting plateau value was obtained at long times in the time dependent self-diffusion coefficient. In each case, $\rho_s = 0.7$ and $kT/\epsilon = 1.0$. The value of D_s for the pure solvent was 0.131 ± 0.002.

ϕ	α	N_c	N_s	m_c/m_s	D_c	η	$10^{-2}K_{B1}$	$10^{-3}K_{B2}$	S
0.1	0.5	10	490	1.000	0.0285	1.22	6.18	2.99	8.94
0.1	0.5	10	490	3.375	0.027*	1.3	1.83	1.36	8.94
0.1	0.5	55	2861	1.000	0.029	1.6	5.82	-	16.1
0.1	0.5	55	2861	3.375	0.0255	1.4	1.76	1.30	16.1
0.1	0.5	100	5224	1.000	0.030	1.3	5.83	-	19.7
0.1	0.5	100	5224	3.375	0.027*	1.3	1.78	1.33	19.7
0.1	1.0	10	854	1.000	0.010	1.6	13.57	-	10.7
0.1	1.0	10	854	8.000	0.012	2.6	4.79	2.35	10.7
0.1	1.0	55	5269	1.000	0.015	1.9	14.39	9.13	19.7
0.1	1.0	55	5269	8.000	0.013*	1.75	1.75	2.42	19.7
0.1	1.0	125	10 851	1.000	0.013	1.7	15.01	-	25.0
0.1	1.5	10	1362	1.000	0.0071	2.4	29.45	24.8	12.5
0.1	1.5	10	1362	3.000	0.0075	3.9	12.49	11.9	12.5
0.1	1.5	10	1362	8.000	0.0072*	3.7*	3.60	5.35	12.5
0.1	1.5	10	1362	15.625	0.008*	3.3	2.32	4.98	12.5
0.1	1.5	50	6862	1.000	0.0076	2.64	31.07	25.4	21.5
0.1	1.5	50	6862	15.625	0.0077*	2.7	1.92	4.25	21.5
0.1	2.0	10	2031	1.000	0.0030	7.2	81.34	76.8	14.3
0.1	2.0	10	2031	5.000	0.003*	8.3	15.45	20.0	14.3
0.1	2.0	10	2031	27.000	0.0044*	7.1*	2.63	8.01	14.3
0.1	2.0	55	10 921	1.000	0.0038	5.4	72.24	72.9	25.0
0.1	2.0	55	10 921	27.000	0.004*	5.9	2.59	7.94	25.0
0.2	0.5	21	479	1.000	0.018	1.65*	6.61	-	8.94
0.2	0.5	122	2794	1.000	0.021	1.65	6.76	3.08	16.09
0.2	0.5	223	5101	1.000	0.020_5	1.76*	6.80	-	19.7
0.3	0.5	204	2712	1.000	0.012	3.25	7.14	3.19	16.1
0.3	0.5	35	465	1.000	0.012	2.63*	7.20	3.21	8.94
0.4	0.5	52	448	1.000	0.0040	4.6	9.21	3.27	8.94
0.4	0.5	305	2611	1.000	0.0030	3.0	7.99	3.02	16.1

loidal particle. Data corresponding to the finite packing fraction simulations are covered in Table II. Table III compares the results from simulations carried out with either the WCA or LJ potentials for the three types of interaction (u_{cc}, u_{cs}, and u_{ss}) but otherwise identical system parameters for some of the α/σ_s and m_c/m_s combinations.

We consider first the simulations with a single colloid particle. Table I reveals that the diffusion coefficient of the colloidal particle shows no mass dependence within the statistical uncertainty associated with averaging for only one particle. This behavior is consistent with the discussion in Sec. II. However, the value of D_c is sensitive to the solvent

TABLE III. Comparisons between the WCA and LJ simulations at $\phi \sim 0.1$. The asterisk denotes that an ambiguous limiting plateau value was obtained in the time dependent self-diffusion coefficient at long times.

α	N_c	N_s	m_c/m_s	D_{WCA}	D_{LJ}	$10^{-2}K_{B1}$ (WCA)	$10^{-2}K_{B1}$ (LJ)	$10^{-3}K_{B2}$ (WCA)	$10^{-3}K_{B2}$ (LJ)
1.5	10	1362	1.000	0.0071	0.0060	29.45	28.1	24.8	20.7
1.5	10	1362	15.625	0.008*	0.0046	2.32	1.80	4.98	4.15
2.0	10	2038	1.000	0.003	0.002	81.3	73.9	76.8	65.8
2.0	55	10921	1.000	0.0038	0.0022	72.2	72.8	72.9	65.5
2.0	55	10921	27.000	0.0040	0.0025	2.59	2.55	7.94	7.39

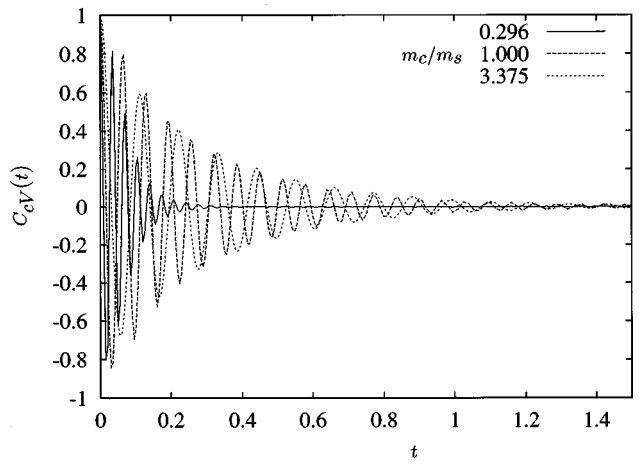

FIG. 1. Colloidal particle velocity autocorrelation functions for WCA simulations carried out with a single colloidal particle with $\alpha=2.5$ and at a solvent density $\rho_s=0.9$, and three colloid masses m_c/m_s given in the figure. $N=8000$. Dimensionless units are used in all of the figures.

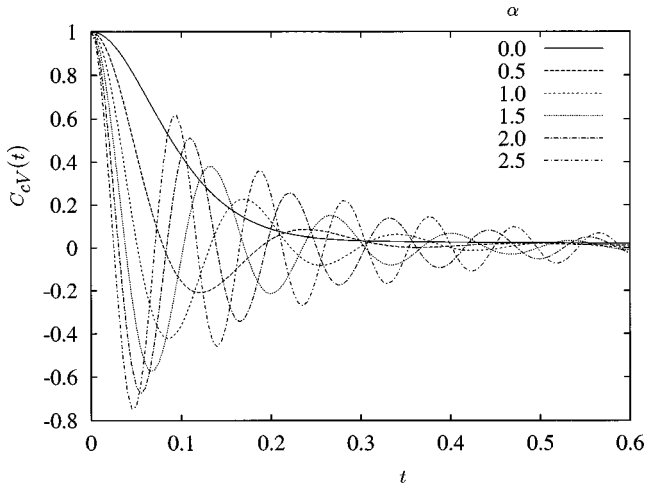

FIG. 3. Colloidal particle velocity autocorrelation functions for WCA simulations carried out with a single colloidal particle taking $\alpha=0.0-2.5$, and at a solvent density $\rho_s=0.7$. The three colloidal particle masses shown are given in the figure. $N=8000$.

density and to the size of the solute particle. The value of D_c decreases with increasing σ_c and ρ_s. Even though D_c does not depend on mass to any noticeable extent, the associated velocity autocorrelation functions (VACF's) are strongly mass dependent, oscillating with a higher frequency but more rapidly damped with decreasing value of m_c. Figure 1 shows the VACF for three values of m_c/m_s for $\alpha=2.5$ and $\rho_s=0.9$. As the mass decreases or equivalently the density of the colloidal particle decreases, the VACF becomes more oscillatory, which indicates a stronger ''backscattering'' of the colloidal particle as it ''rattles'' in its solvent cage. As the density of the colloidal particle decreases, it oscillates within its cage with increasing frequency, becoming more decoupled from the surrounding solvent dynamics (at least at short time). Figure 2 shows the corresponding time dependent diffusion coefficients $D_c(t)$, which are seen not to be mass dependent within the statistical uncertainty of the simulations. For a constant mass of the colloidal particle its density decreases drastically through $\alpha=0.5-2.5$ when compared with that of the solvent particle [as the density of the colloidal particle is $\sim m_c(\sigma_s/(\sigma_s+2\alpha))^{-3}$]. Although the colloidal particle becomes large compared to the solvent particle the colloid particle dynamics become dominated by the surrounding solvent molecules at long times. The VACF also become more oscillatory as the size of the colloidal particle increases, keeping the mass the same (see Fig. 3) for α in the range 0.0–2.5 and with $m_c/m_s=1$. Figure 4 shows that the self-diffusion coefficients decrease with increasing colloidal particle size.

An estimate of the time scale at which the solvent becomes influential on the velocity relaxation of the colloidal particle can be made by comparing the colloid normalized VACF with the function $\cos(\Omega_{c0}t)$, where Ω_{c0} is the Einstein frequency of the colloidal particle, computed in each case from the first Mori coefficient K_{c1}. Figure 5 compares the normalized VACF for a mass $m_c/m_s=0.296$ at $\rho_s=0.7$ and $\alpha=0.5$ with $\cos(\Omega_{c0}t)$. The short-time behavior of the VACF is given accurately by this function for all α and m_c/m_s considered. This agreement extends further out in time for the less massive colloidal particles. The VACF looks typi-

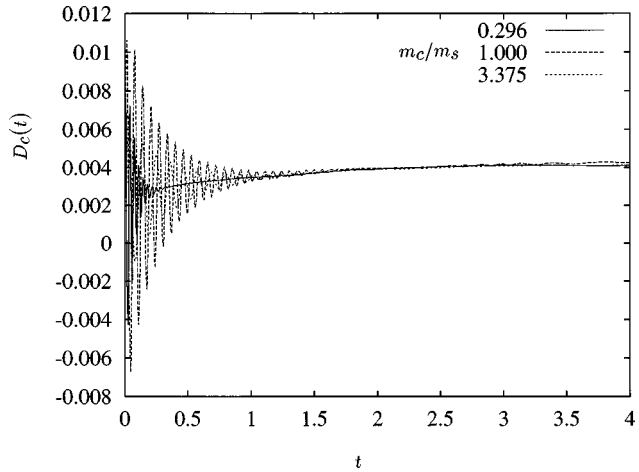

FIG. 2. The derived time-dependent self-diffusion coefficients of the colloidal particles using Eq. (2) and the VACF of Fig. 1.

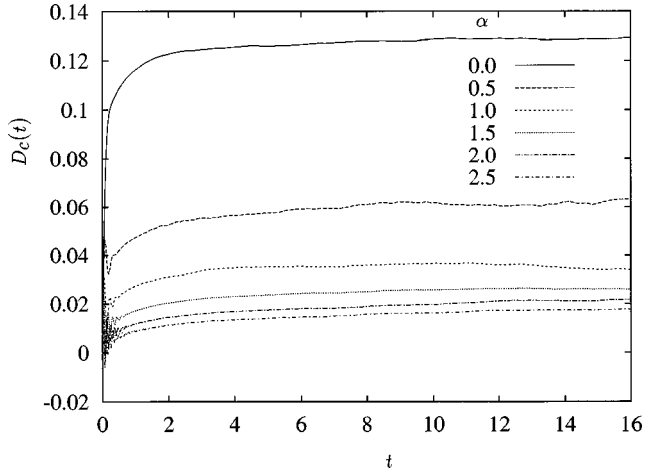

FIG. 4. The derived time-dependent self-diffusion coefficients using Eq. (2) and the VACF shown in Fig. 3.

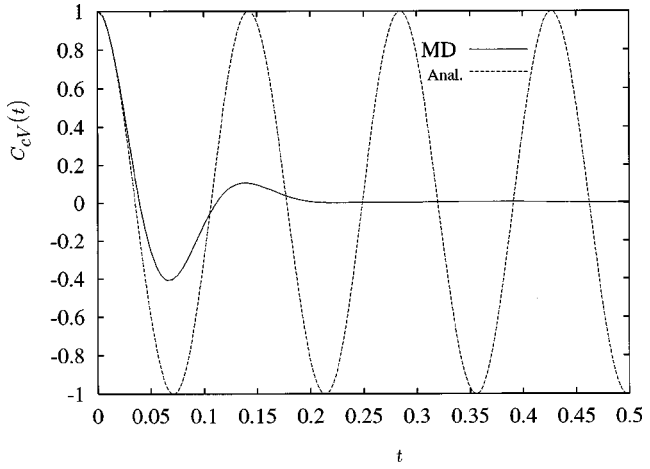

FIG. 5. Comparison between $C_{Vc}(t)$, with $\cos(\Omega_{c0}t)$ for the state points $\rho_s=0.7$, $\alpha=0.5$, $N=8000$, and $m_c/m_s=0.296$.

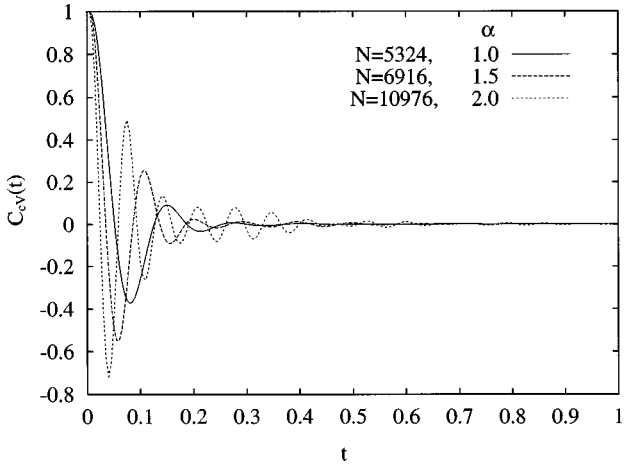

FIG. 7. As for Fig. 6, except that the α dependence is considered at a fixed colloidal particle mass of $m_c/m_s=1.0$.

cally like that of a damped harmonic oscillator which gradually loses its initial phase after many oscillations, and decays in a nonexponential fashion. As the density of the colloidal particle approaches that of the solvent particle, the point of departure between the two functions moves to shorter times. This reflects a better degree of coupling between the dynamics of colloid and solvent molecule. The same trend is apparent on reducing the colloidal particle size toward that of the solvent, while the mass of the colloidal particle is kept constant. Classical solutions of the Langevin equation also predict an effect of colloid particle density on its velocity autocorrelation function [28–30]. However, they do not capture the negative regions in the VACF characteristic of collisional ''rebound'' effects, which are so prominent in the systems studied here. This is not surprising as the Langevin equation does not take account of the microstructure of the solvent and nanocolloid system, which is essential if collisional effects are to be reproduced. Much larger, μm-sized, colloidal particles are probably required for these formulas to be accurate representations of the colloidal dynamics.

We turn now to the simulations carried out with more than one colloidal particle in the simulation cell. Figure 6 shows that there is an increasing oscillation frequency with decreasing colloid mass for the $\phi=0.1$ and $\rho_s=0.7$ systems for m_c/m_s in the range 1.0–15.6 and $\alpha=1.5$. Figure 7 shows the effect of colloid particle size on the VACF for

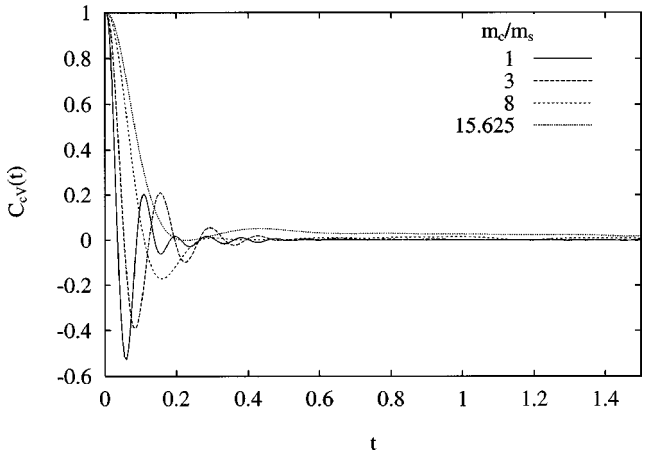

FIG. 6. Colloidal particle velocity autocorrelation functions for WCA simulations carried out with ten colloidal particles taking $\alpha=1.5$ and at a solvent density $\rho_s=0.7$. The four colloidal particle masses considered are shown are in the figure. $N=1372$. The mass ratios m_c/m_s are given on the figure.

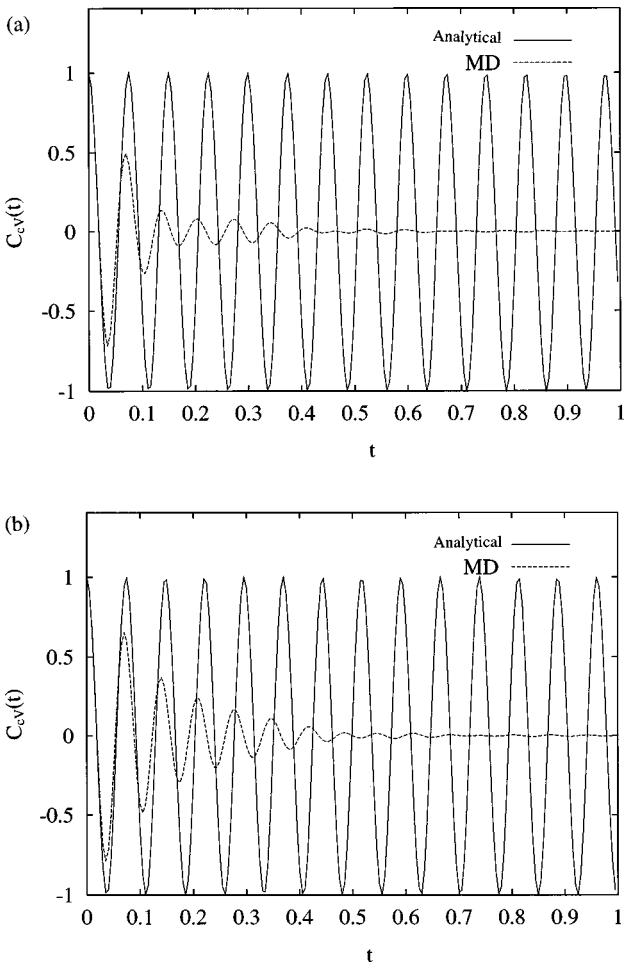

FIG. 8. Colloidal particle velocity autocorrelation functions for (a) WCA and (b) LJ simulations carried out with 55 colloidal particles and 10 921 solvent molecules taking $\alpha=2.0$ and at solvent densities $\rho_s=0.7$ and $m_c/m_s=1.0$.

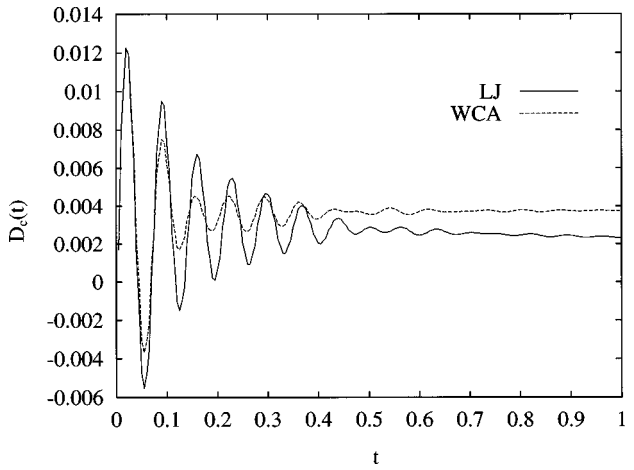

FIG. 9. The time dependent self-diffusion coefficient of two simulations carried out with WCA and LJ potentials. $\alpha=2.0$, $m_c/m_s=1.0$, $N_c=55$, and $N_s=10\,921$.

$m_c/m_s=1$. Again as for the infinite dilution systems, the oscillation frequency increases with particle size. Therefore, the same trends in the VACF are apparent in simulations carried out at finite colloid packing fractions, with the Einstein frequency again accounting for the short-time decay of the VACF (in this case it includes the effects of mass, size, and concentration of colloidal particles) [see Fig. 8, where there is again short time coincidence between the colloidal normalized VACF and $\cos(\Omega_{c0}t)$].

Additional simulations were carried out using the LJ potential with an interaction truncation distance of $r_{co}=2.5r_m$ in order to discover the effect of the type and range of the potential. Parameters and results from these simulations are compared with those of the equivalent WCA potential in Table III. Figures 8 and 9 show the VACF and integrated VACF's, respectively, for comparable WCA and LJ systems at finite packing fraction. The LJ function oscillates at the same frequency as that of the WCA system. This is to be expected as the first and second Mori coefficients of the two systems are the same within the simulation statistics (see

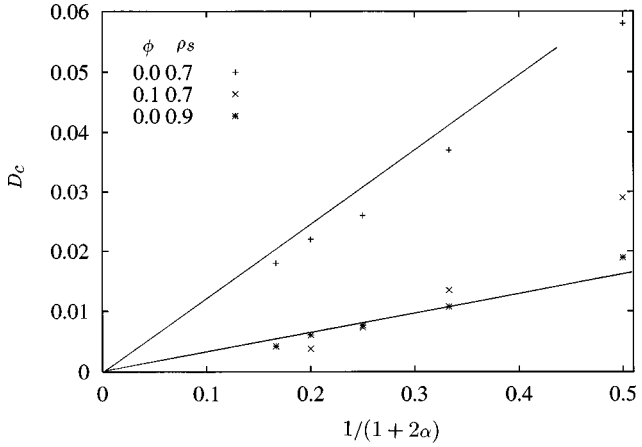

FIG. 10. Dependence of the colloid self-diffusion coefficient on the colloidal particle diameter $(\sigma_s+2\alpha)^{-1}$ for two volume fractions and solvent densities. The lines correspond to the predicted slopes based on the Stokes-Einstein relationship [Eq. (22)] for the $\phi\rightarrow 0$ systems.

TABLE IV. Mean values for the self-diffusion coefficient for the WCA systems described in Table II using $\alpha=0.5$ and $\rho_s=0.7$. The Einstein and experimentally derived expressions are from Eqs. (23) and (24), which are denoted by $(D/D_0)_1$ and $(D/D_0)_2$, respectively, in the table heading. We use $D_0=0.058$ to scale the simulation data (MD). The heading $(D/D_0)_{MD}$ denotes the ratio obtained from the simulations.

ϕ	D	$(D/D_0)_{MD}$	$(D/D_0)_1$	$(D/D_0)_2$
0.1	0.029	0.50	0.75	0.57
0.2	0.021	0.36	0.50	0.37
0.3	0.012	0.21	0.25	0.21
0.4	0.004	0.07	0.00	0.09

Table III). Nevertheless, the amplitude of the LJ system is larger and the limiting self-diffusion coefficient is lower. Therefore although the harmonic frequencies of the velocity relaxation are statistically the same, the relaxation of the colloidal particles within the cage at later times is different. Presumably, the surrounding cage is more ''rigid'' in the case of LJ fluid, which acts as a better restraint on the central particle, making its correlation function retain its oscillatory form for longer time and causing the diffusion coefficient to be lower than in the WCA case. Coincidence of the short-time behavior of the VACF of the WCA and LJ pure fluids was also noted by Dean and Kushick [31].

The diffusion coefficient of the colloidal particle is sensitive to the size of the colloidal particle and solvent bulk density. For self-diffusion the classical solution for macroscopic spheres at infinite dilution is

$$D_c=\frac{kT}{3\pi\sigma_c\eta_0} \tag{22}$$

if we assume stick boundary conditions, and η_0 is the shear viscosity of the bulk solvent, which can be obtained using the Green-Kubo formula for example. Figure 10 gives a plot of D against σ_c^{-1}, where $\sigma_c=\sigma_s+2\alpha$ at two volume fractions and solvent densities. At infinite dilution, the data fall on a straight line for the larger particle size range with a $D_c=0$ intercept at infinite dilution. The slopes of the $\rho_s=0.7$ and 0.9 systems are in reasonable agreement with the predictions based on Eq. (22), which are also given in Fig. 10. The reduced values of the self-diffusion coefficients at finite volume fraction make it more difficult to obtain a reliable extrapolation. The D_c for the $\alpha=0.5$ WCA system states (Table IV) decrease almost linearly with increasing ϕ over the whole packing fraction range. The volume fraction dependence of the colloid self-diffusion to first order is given by the Einstein-Batchelor formula [1]

$$\frac{D_c(\phi)}{D_{c0}}=1-2.5\phi+\cdots, \tag{23}$$

where D_c and D_{c0} are the self-diffusion coefficients of colloidal particles at long time and infinite dilution (i.e., $N_c=1$), respectively. An accurate fit to experimental data covering the higher volume fraction region is given by Eq. (24), [32],

TABLE V. Mean value for the shear viscosity η for the WCA systems of Table II using $\alpha=0.5$ and $\rho_s=0.7$. The η/η_0 were calculated using $\eta_0=0.84$ from Table I. The predictions from Eqs. (25) and (26) are denoted by $(\eta/\eta_0)_1$ and $(\eta/\eta_0)_{\mathrm{KD}}$, respectively. The standard errors are typically $\sim 10\%$. The heading $(\eta/\eta_0)_{\mathrm{MD}}$ denotes the ratio obtained from the simulations.

ϕ	η	$(\eta/\eta_0)_{\mathrm{MD}}$	$(\eta/\eta_0)_1$	$(\eta/\eta_0)_{\mathrm{KD}}$
0.1	1.35	1.6	1.31	1.41
0.2	1.69	2.0	1.74	2.15
0.3	2.94	3.5	2.29	3.64
0.4	3.80	4.5	2.96	7.50

$$\frac{D_c(\phi)}{D_{c0}}=0.8(1.00-1.15\phi)(1.0-2.0\phi). \tag{24}$$

Table IV shows that the prediction for D_c/D_{c0} from Eq. (23) overestimates the value for D_c/D_{c0} at finite packing fraction (especially at $\phi=0.1$). The agreement with the simulation data is much better using Eq. (24).

The shear viscosity of the model colloidal liquids was also computed using the shear stress correlation function and the appropriate Green-Kubo formula [13]. Let η be the viscosity of the colloidal mixture. The values computed are presented in Tables I and II. Both D and η were subject to greater statistical uncertainty with increasing packing fraction and colloidal particle size, and sometimes it was difficult to establish a level plateau in the respective integrated time correlation functions. Nevertheless, the expected trend of increasing shear viscosity with volume fraction was observed (see Table III). The value of the viscosity decreased with increasing system size, presumably because the collection of molecules was less constrained by the periodic boundary conditions for larger systems, and therefore the ''activation'' energies for transitions between the various configurational states were typically lower. The mass dependence was not studied at the higher packing fractions for $\phi>0.1$. As the number of colloidal particles increased, the coarse-grained nature of the solvent was probably contributing to the greater statistical fluctuation in the data. Phase space became more structured and the system was probably more readily ''trapped'' in only part of the available phase space for times comparable to the length of the simulation. A low order expansion for the ratio η/η_0 according to classical hydrodynamics is [1]

$$\frac{\eta(\phi)}{\eta_0}=1+2.5\phi+(6\pm 1)\phi^2+\cdots. \tag{25}$$

The Krieger-Docherty expression is an empirical formula which covers the higher end of the colloidal liquid range, and which is in reasonable agreement with existing experimental data in the range covered here [1],

$$\frac{\eta(\phi)}{\eta_0}=\frac{1}{(1-\phi/\phi_m)^2}\approx 1+\frac{2}{\phi_m}\phi+\cdots, \tag{26}$$

where the random close packing fraction is at $\phi_m=0.63$. It is clear from the values in Table V that agreement with simulation data is best with Eq. (26), although the viscosity is systematically lower than found experimentally [represented well by Eq. (26)], particularly with increasing volume fraction. Nevertheless, the agreement between the simulated and experimental self-diffusion coefficients and the shear viscosity is quite remarkable, as these model colloidal particles are rather small. It suggests that the volume fraction dependence of the Newtonian shear viscosity observed for macrocolloidal particle systems may extend largely unchanged down to simple liquid distance scales.

V. CONCLUSIONS

We have investigated the self-diffusion coefficients and shear viscosity of model nanocolloidal dispersions. The mass and size dependence of the VACF's were calculated. For colloidal particles with a lower density than the solvent molecules, the colloidal VACF had a pronounced damped oscillatory form with a frequency given well by the Einstein frequency Ω_{c0}. The oscillatory frequency increased with decreasing mass and increasing solvent density. Both of these parameters (and also the value of the colloid concentration) determined the value of the first Mori coefficient of the colloidal particle (K_{c1}) and also the oscillation frequency ($\Omega_0=\sqrt{K_{c1}}$) to a very good approximation.

Despite the oscillations observed in the VACF for small mass colloidal particles, the influence of colloid particle density on the value of the self-diffusion coefficient was found to be remarkably small. The self-diffusion coefficients were sensitive to colloid particle size however, but not to mass at a given size. Additional simulations were carried out using the LJ form for all interactions in the system. The first Mori coefficients of the WCA and LJ systems were statistically the same for equal colloidal particle size and solvent density, and, consistent with this, the oscillation frequency in the velocity autocorrelation function was the same in both cases. The amplitude of the oscillations was larger for the LJ systems and self-diffusion coefficients were smaller, reflecting the greater cohesion of the LJ fluid, which acted to restrain better the colloidal particle (even though the force field experienced by the colloidal particle was much the same). The Stokes-Einstein formula for the self-diffusion coefficient at infinite dilution applies well even for these small colloidal particles, especially for the higher liquid number densities.

The concentration dependence of the self-diffusion coefficients and the shear viscosity agreed quite well with classical limiting and semiempirical expressions derived from experimental data for much larger colloidal particles, suggesting a wider range of colloidal particle sizes where these formulas can be applied. A possible additional interest in the mass dependence of these colloidal particles may be found for the larger and lower density colloidal particles, which increasingly resemble a vapor cavity in the liquid. Vapor cavities are of some current research interest as they occur in cavitating liquids and other areas of practical interest (e.g., in foams).

ACKNOWLEDGMENTS

This project was partly supported by the Spanish DGICYT (Project No. PB95-0254) and by Junta de Extremadura

(Consejería de Educación y Juventud). The authors thank the British Council and Delegación de Investigación y Ciencia for supporting this work under the Collaboration Project (Acciones Integradas) between the U.K. and Spain. The Engineering and Physical Sciences Research Council of Great Britain (EPSRC) is thanked for providing computer workstations in the Department of Chemistry, University of Surrey, upon which some of these calculations were carried out.

[1] W. B. Russel, D. A. Saville, and W. R. Schowalter, *Colloidal Dispersions* (Cambridge University Press, Cambridge, 1989).
[2] D. L. Ermak, J. Chem. Phys. **62**, 4189 (1975).
[3] D. L. Ermak and J. A. McCammon, J. Chem. Phys. **69**, 1352 (1978).
[4] L. Durlofsky, J. F. Brady, and G. Bossis, J. Fluid Mech. **180**, 21 (1987).
[5] A. J. C. Ladd, J. Chem. Phys. **93**, 3484 (1990).
[6] B. Cichocki, B. U. Felderhof, K. Hinsen, E. Wajnryb, and J. Blawzdziewicz, J. Chem. Phys. **100**, 3780 (1994).
[7] L. E. Silbert, J. R. Melrose, and R. C. Ball, Phys. Rev. E **56**, 7067 (1997).
[8] L. F. Rull, E. de Miguel, J. J. Morales, and M. J. Nuevo, Phys. Rev. A **40**, 5856 (1989).
[9] J. J. Morales and M. J. Nuevo, J. Comput. Chem. **13**, 1119 (1992).
[10] M. J. Nuevo and J. J. Morales, Phys. Lett. A **178**, 114 (1993).
[11] M. J. Nuevo, J. J. Morales, and D. M. Heyes, Phys. Rev. E **51**, 2026 (1995).
[12] M. J. Nuevo, J. J. Morales, and D. M. Heyes, Phys. Rev. E **55**, 4217 (1997).
[13] M. P. Allen and D. J. Tildesley, *Computer Simulation of Liquids* (Clarendon, Oxford, 1987).
[14] K. Tankeshwar, J. Phys.: Condens. Matter **7**, 9715 (1995).
[15] R. K. Sharma, K. Tankeshwar, and K. N. Pathak, J. Phys.: Condens. Matter **7**, 537 (1995).
[16] J.-P. Hansen and I. R. McDonald, *Theory of Simple Liquids*, 2nd ed. (Academic, London, 1986).
[17] B. J. Berne and G. D. Harp, Adv. Chem. Phys. **17**, 63 (1970).
[18] H. Mori, Prog. Theor. Phys. **33**, 423 (1965); **34**, 399 (1965).
[19] L. L. Lee, Physica A **100**, 205 (1980).
[20] S. Toxvaerd, J. Chem. Phys. **81**, 5131 (1984).
[21] S. Toxvaerd, Mol. Phys. **56**, 1017 (1985).
[22] J. D. Weeks, D. Chandler, and H. C. Andersen, J. Chem. Phys. **54**, 5237 (1971).
[23] L. Verlet, Phys. Rev. **159**, 98 (1967).
[24] L. V. Woodcock, Chem. Phys. Lett. **10**, 257 (1971).
[25] S. Toxvaerd, Mol. Phys. **72**, 159 (1991).
[26] S. Nosé, Mol. Phys. **52**, 255 (1984).
[27] W. G. Hoover, Phys. Rev. A **31**, 1695 (1985).
[28] E. J. Hinch, J. Fluid Mech. **72**, 499 (1975).
[29] D. A. Weitz, D. J. Pine, P. N. Pusey, and R. J. A. Tough, Phys. Rev. Lett. **63**, 1747 (1989).
[30] P. Espagñol and I. Zúñiga, Int. J. Mod. Phys. B **9**, 469 (1995).
[31] D. P. Dean and J. N. Kushick, J. Chem. Phys. **76**, 619 (1982).
[32] D. M. Heyes, J. Phys.: Condens. Matter **7**, 8857 (1995).